PCCP

Physical Chemistry Chemical Physics

www.rsc.org/pccp

Volume 12 | Number 31 | 21 August 2010 | Pages 8649–9108

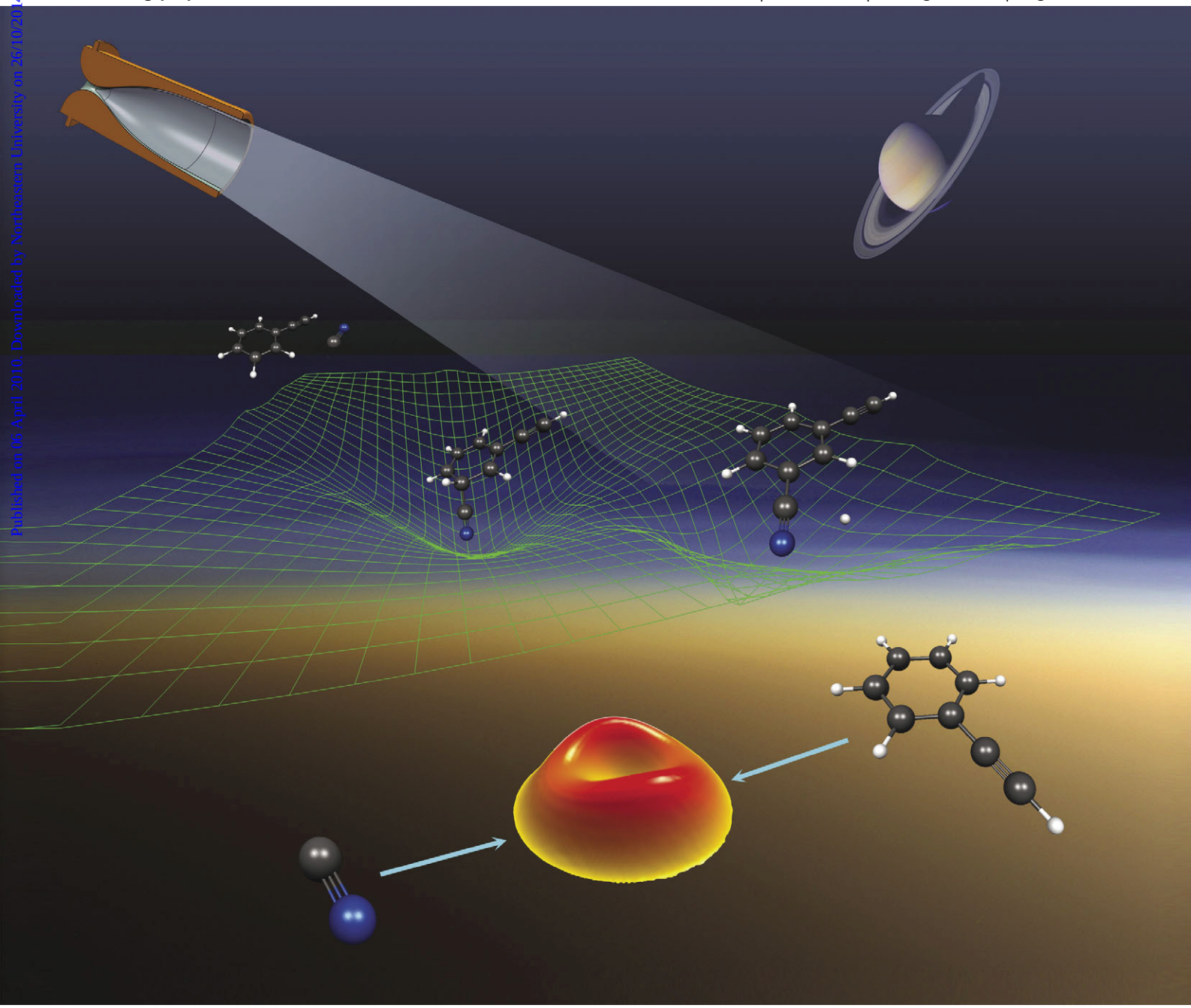

ISSN 1463-9076

COVER ARTICLE
Kaiser *et al.*
A chemical dynamics, kinetics, and theoretical study on the reaction of the cyano radical with phenylacetylene

HOT ARTICLE
Wang
Covalent gold

1463-9076(2010)12:31;1-#

A chemical dynamics, kinetics, and theoretical study on the reaction of the cyano radical (CN; $X^2\Sigma^+$) with phenylacetylene (C_6H_5CCH; X^1A_1)†

Chris J. Bennett,‡[a] Sébastien B. Morales,§[a] Sébastien D. Le Picard,[a] André Canosa,[a] Ian R. Sims,*[a] Y. H. Shih,[b] A. H. H. Chang,[b] Xibin Gu,[c] Fantong Zhang[c] and Ralf I. Kaiser*[c]

Received 30th November 2009, Accepted 26th February 2010
DOI: 10.1039/b925072g

The chemical reaction dynamics to form *o*-, *m*-, and *p*-cyanophenylacetylene *via* the neutral–neutral reaction of ground state cyano radicals with phenylacetylene and D_1-phenylacetylene were investigated in crossed beam experiments; these studies were combined with kinetics measurements of the rate coefficients at temperatures of 123, 200, and 298 K and supplemented by electronic structure calculations. The data suggest that the reaction is initiated by a barrier-less addition of the electrophilic cyano radical to the *o*-, *m*-, or *p*-position of the aromatic ring. The eventually fragmented *via* atomic hydrogen elimination to form *o*-, *m*-, and *p*-cyanophenylacetylene *via* tight exit transition states with the hydrogen atom being ejected almost perpendicularly to the molecular plane of the rotating complex. The overall reaction to form *o*-, *m*-, and *p*-cyanophenylacetylene was found to be exoergic by 89 ± 18 kJ mol^{-1} in nice agreement with the calculations. The *o*-cyanophenylacetylene isomer is of particular relevance as a potential building block to the formation of nitrogen-substituted didehydronaphthalene molecules in analogy to didehydronaphthalene in Titan's aerosol layers—a pathway hitherto neglected by the planetary science modeling community.

1. Introduction

The chemical kinetics and dynamics of small radical reactions with unsaturated hydrocarbons are of paramount importance in understanding the formation of polycyclic aromatic hydrocarbons (PAHs) together with their hydrogen deficient precursors from the 'bottom up' in combustion processes,[1] in the interstellar medium[2,3] and in our Solar System.[4] A better knowledge of the reactions of ground state cyano radicals, $CN(X^2\Sigma^+)$, is particularly valuable to understand the synthesis of complex nitriles in hydrocarbon-rich atmospheres of planets and their moons—predominantly of Saturn's moon Titan.[5–7] Unsaturated hydrocarbons and their nitriles are thought to be key intermediates to form Titan's organic, aerosol-particle based haze layers. These haze layers are of basic significance to Titan's chemistry since they absorb the destructive ultraviolet radiation to protect astrobiologically important molecules from being destroyed in the lower parts of the atmosphere,[8] act as anti-greenhouse species to control the radiation and temperature balance,[9] and influence Titan's weather system[10,11] Here, the cyano radical is considered as the key radical involved in the formation of these nitriles. Whereas the main source of the cyano radicals has been unambiguously identified as the photolysis of hydrogen cyanide (HCN),[12–16] the underlying dynamics of cyano radical reactions and their role in the build-up of complex nitriles have only begun recently to be understood as a result of a series of detailed experiments on the elementary steps of cyano radical reactions with unsaturated hydrocarbon molecules (Fig. 1).[17] Reaction kinetics experiments at temperatures as low as 15 K showed that cyano radical reactions with unsaturated hydrocarbons such as acetylene, ethylene and methyl acetylene are fast (2–5 × 10^{-10} cm^3 s^{-1}) and proceed without entrance barriers.[18,19] These high rate constants at the low temperatures of Titan's atmosphere present a crucial prerequisite to form organic nitriles.

Here, we expand our studies and investigate the dynamics and kinetics of the reaction of cyano radicals with phenylacetylene. It has been suggested that the isoelectronic reaction of ethynyl radicals with phenylacetylene is of crucial importance to form aromatic molecules incorporating the naphthalene core (Fig. 2, panel a). Initiated by a barrier-less addition of the ethynyl radical (C_2H) to the *ortho* carbon atom of the phenylacetylene (C_6H_5CCH) molecule [1] (Fig. 2), the reactive intermediate rapidly loses a hydrogen atom forming 1,2-diethynylbenzene [2].[20] The latter could react with a second ethynyl radical through addition to a carbon atom of one of the ethynyl side chains yielding a doublet radical intermediate [3]. A consecutive ring closure of the intermediate leads to an ethynyl-substituted naphthalene core [4]. This core ejects a hydrogen atom to form ethynyl-substituted

[a] *Institut de Physique de Rennes, Equipe: "Astrochimie Expérimentale", UMR UR1-CNRS 6251, Université de Rennes 1, Campus de Beaulieu, 35042 Rennes Cedex, France. E-mail: ian.sims@univ-rennes1.fr*
[b] *Department of Chemistry, National Dong Hwa University, Hualien, Taiwan*
[c] *Department of Chemistry, University of Hawaii at Manoa, Honolulu, USA. E-mail: ralfk@hawaii.edu*

† Electronic supplementary information (ESI) available: Additional experimental details. See DOI: 10.1039/b925072g

‡ Visiting scientist, permanent address: Department of Chemistry, University of Hawaii at Manoa, Honolulu, HI, USA.
§ Contributed equally to this work.

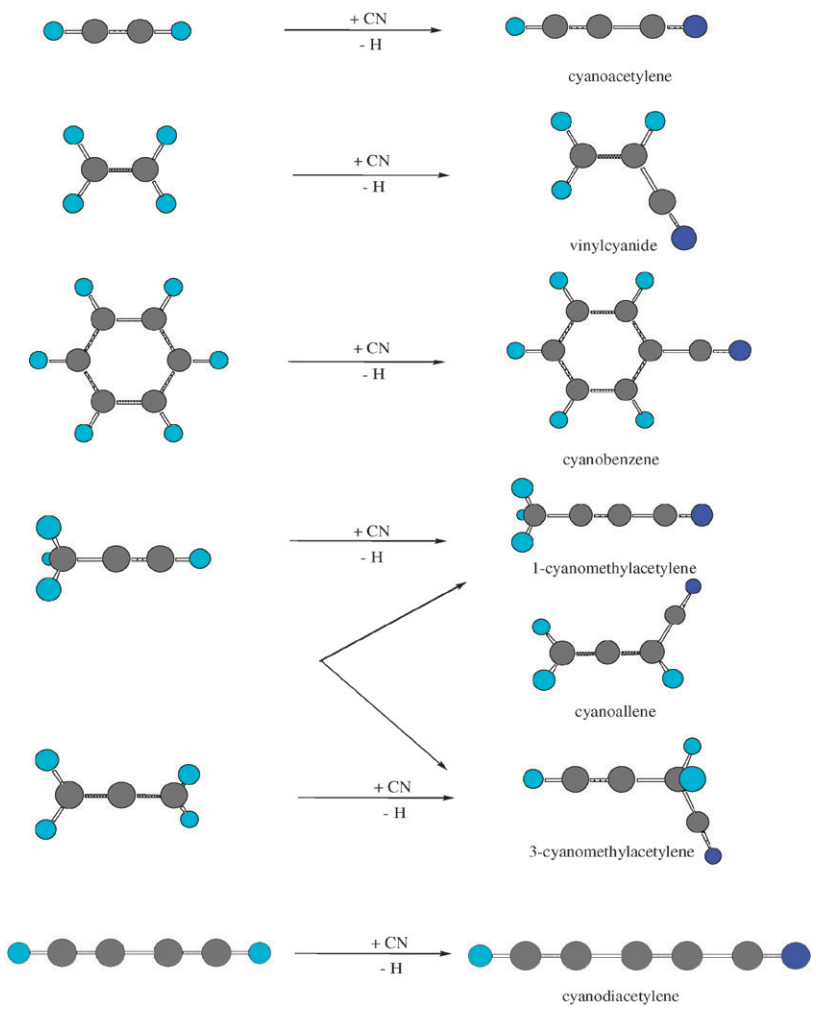

Fig. 1 Nitriles formed in barrier-less reactions of cyano radicals with unsaturated hydrocarbons relevant to the chemistry in the atmosphere of Saturn's moon Titan.

1,2-didehydronaphthalene [5]. In low temperature atmospheres, this ethynyl addition mechanism presents a compelling alternative to high-temperature based hydrogen-abstraction–acetylene addition (HACA) sequences to form polycyclic aromatic hydrocarbon-like species in combustion flames.[21] An alternative reaction sequence could also be initiated by cyano radical reactions with phenylacetylene yielding ultimately a nitrogen-substituted naphthalene core (Fig. 2, panel b). In Titan's atmosphere, this would effectively couple the hydrocarbon with the nitrogen chemistries. However, the very first step in this reaction sequence is the hitherto unexplored reaction of cyano radicals with phenylacetylene.

Therefore, to better understand the dynamics and kinetics of the reaction of cyano radicals with phenylacetylene in Titan's atmosphere, we conducted a crossed molecular beams investigation of this reaction. To ascertain the position of the atomic hydrogen loss, *i.e.* the benzene ring *versus* the acetylenic unit, we also carried out reactions with D_1-phenylacetylene. This study provided the nature of the reaction product and information on the dynamics. To acquire complementary data on the low temperature rate constants (recall that in the modeling of atmospheres of planets and their moons, reaction products and rate constants are needed), the kinetics of cyano radical reactions with phenylacetylene were probed *via* low temperature kinetics studies. All experimental findings were finally combined with theoretical data obtained from electronic structure calculations on this reaction. This dynamics, kinetics, and theoretical investigation presents a comprehensive study of the important cyano radical–phenylacetylene system and helps to elucidate implications to the chemical evolution of Titan's atmosphere. These results are compared to those obtained in the crossed beams experiments of cyano radicals with benzene [22] and acetylene.[23]

2. Experimental and theoretical methods

2.1 Crossed beam experiments

Reactive scattering experiments were conducted in a crossed molecular beams machine at The University of Hawai'i. The experimental setup is described in ref. 24 in detail. Briefly, a pulsed supersonic cyano radical beam, $CN(X^2\Sigma^+)$, was produced *in situ* in the primary source chamber *via* laser ablation of graphite at 266 nm at pulse energies of 13–20 mJ and reaction of the ablated species with neat nitrogen gas (99.9999%; Gaspro); molecular nitrogen also acts as a seeding

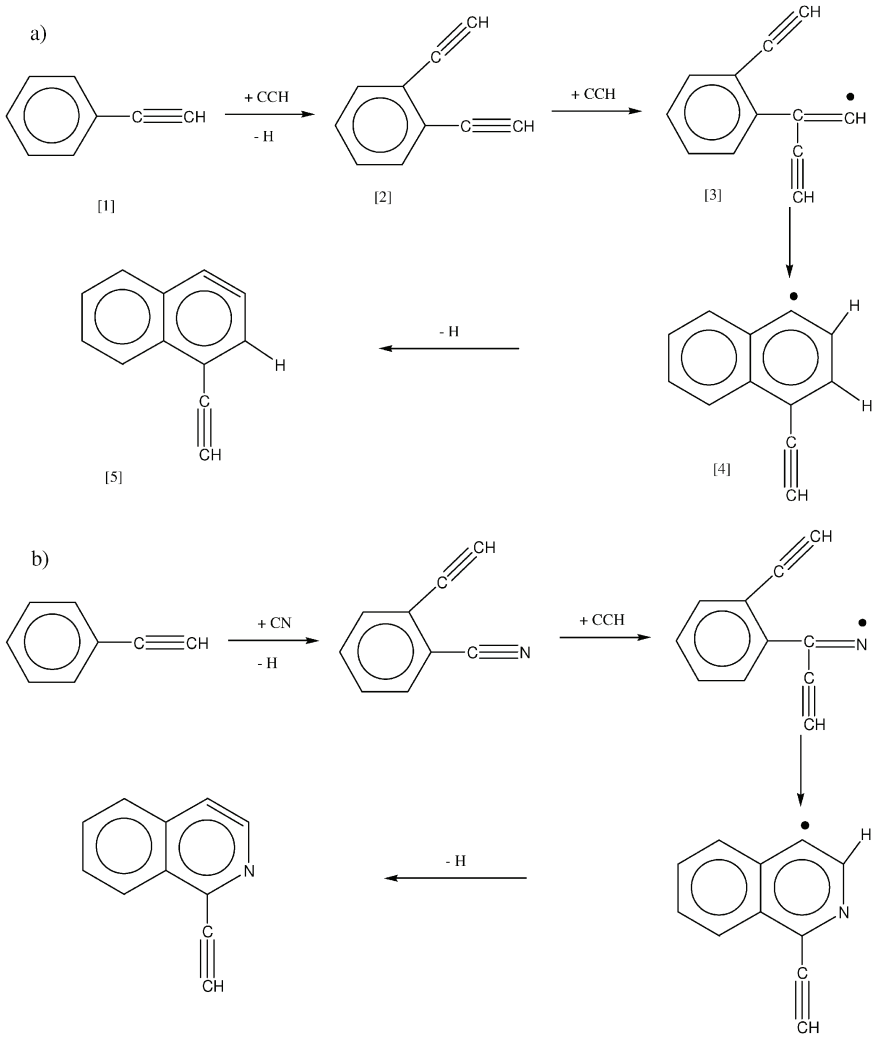

Fig. 2 Schematic representation of the reaction of ethynyl radicals with phenylacetylene to form the naphthalene core. A reaction of isoelectronic cyano radicals with phenylacetylene could lead to nitrogen-substituted PAH like species.

gas of the cyano radicals.[25] After passing a skimmer, a four-slot chopper wheel selected a part of the cyano radical beam with a peak velocity, v_p, of 1628 ± 34 m s^{-1} and a speed ratio, S, of about 3.1 ± 0.2. This radical beam intersected a pulsed phenylacetylene (99.9%+; Aldrich) or D_1-phenylacetylene (99.5%+D; Aldrich) beam seeded in argon carrier gas (99.9999%; Gaspro) at fractions of 1 to 2% released by a second pulsed valve at a well-defined collision energies of 31.2 ± 1.3 and 30.9 ± 1.7 kJ mol^{-1}, respectively. In D_1-phenylacetylene, the deuterium atom is located at the acetylenic carbon atom. Peak velocities of the secondary beams were 598 ± 15 m s^{-1} for both the phenylacetylene and D_1-phenylacetylene beams at speed ratios of 28 ± 2. This resulted in center-of-mass angles of 55.2° ± 1.2° and 55.7° ± 1.4° for phenylacetylene and D_1-phenylacetyelene, respectively. Note that the primary beam contains, besides the cyano radical, carbon atoms as well as dicarbon and tricarbon molecules. However, we demonstrated that tricarbon molecules have a significant entrance barrier upon reacting with a range of unsaturated hydrocarbon molecules of at least 45 kJ mol^{-1}.[26] Therefore, tricarbon does not react with phenylacetylene under our experimental conditions. On the other hand, dicarbon molecules and carbon atoms have masses of 24 and 12 atomic mass units, respectively, compared to 26 atomic mass units for the cyano radical. Therefore, carbon and dicarbon molecules lead to products upon reaction with phenylacetylene which are *lower* in mass than those formed in the reaction of cyano radicals. Therefore, neither dicarbon nor carbon atoms interfered in the reactive signals observed.

Reactively scattered products were monitored using a quadrupole mass spectrometric detector in the time-of-flight (TOF) mode after electron-impact ionization of the molecules at 80 eV with an emission current of 2 mA. The detector is rotatable within the plane defined by the primary and the secondary reactant beams to take angular resolved TOF spectra. By integrating the TOF spectra at the laboratory angles and correcting for the day-to-day intensity fluctuations of the cyano radical beam, the laboratory angular distribution was obtained. The latter plots the integrated intensity of an ion of distinct mass-to-charge (m/z) *versus* the laboratory angle. Information on the chemical dynamics was gained by fitting

these TOF spectra and the angular distribution in the laboratory frame (LAB) using a forward-convolution routine.[27] This approach initially presumes the angular flux distribution $T(\theta)$ and the translational energy flux distribution $P(E_T)$ in the center-of-mass system (CM) assuming mutual independence. TOF spectra and the laboratory angular distributions are then calculated from these $T(\theta)$ and $P(E_T)$ convoluted over the apparatus functions to obtain simulations of the experimental data. The essential output of this fitting routine is a product flux contour map, $I(\theta,u) = P(u) \times T(\theta)$, which plots the intensity of the reactively scattered products (I) as a function of the center-of-mass scattering angle (θ) and product velocity (u). This map can be seen as the *image* of the chemical reaction and contains *all* the information on the scattering process. Since previous kinetics studies of cyano radical reactions with benzene and acetylene showed the absence of an entrance barrier to reaction,[22,23] we included an energy dependent cross-section, $\sigma(E_c) \approx E_C^{-1/3}$, with the collision energy E_C.[28] Finally, it should be mentioned that due to the low signal counts, we had to record up to 2.6×10^6 TOF spectra to obtain a good signal to noise ratio of the reactively scattered species.

2.2. Kinetics experiments

Rate coefficients were measured for the reaction of cyano with phenylacetylene at temperatures of 123, 200, and 298 K. A full description of the CRESU apparatus has been given elsewhere. Furthermore, the methods used to study the kinetics of this reaction closely follow those used previously for cyano radical reactions.[18,19,29,30] Briefly, in the CRESU technique, a cold gas-phase environment is created by isentropic expansion of a buffer gas (He, Ar or N_2) through an axisymmetric Laval nozzle,[31] into a chamber coupled to a very high capacity pumping system. The resulting uniform supersonic flow provides a very low temperature gas-phase environment (currently down to 15 K with no precooling) while avoiding condensation even of species that are not very volatile at room temperature. The technique is combined with pulsed laser photolysis–laser-induced fluorescence (PLP-LIF) technique to study reaction kinetics at these low temperatures. Measurements at temperatures lower than 123 K were not possible in this study for reasons discussed below.

Cyano radicals in their $X^2\Sigma^+$ ground electronic state were generated as in Carty *et al.*[19] by the photolysis of iodocyanide (ICN; Aldrich, 95%) at 266 nm using the fourth harmonic output of a 10 Hz pulsed Nd:YAG laser (Spectra Physics GCR 190) at a fluence in the reaction zone of $\sim$80 mJ cm^{-2}. A small flow (a few standard cm^3 min^{-1}) of helium was passed over crystals of ICN before this flow of gas entered the gas reservoir upstream of the Laval nozzle. Photodissociation of ICN at this wavelength produces CN radicals that are overwhelmingly in the $v = 0$ level of the $X^2\Sigma^+$ ground vibronic state, but over a wide range of rotational levels.[32] Cyano radicals were detected by exciting them in the (0,0) band of the CN ($B^2\Sigma^+$–$X^2\Sigma^+$) system at $\sim$388 nm using the doubled idler output of a tunable optical parametric oscillator (Spectra Physics MOPO), pumped by the tripled output of another Nd:YAG laser (Spectra Physics GCR 230). Fluorescence in the (0,1) band at $\sim$420 nm was collected *via* an appropriate combination of a UV-enhanced mirror and fused silica lenses onto the photocathode of a UV sensitive photomultiplier tube (Thorn EMI) through a narrow band interference filter centered at 420 nm with a 10 nm FWHM bandwidth (Ealing Optics). Tests were carried out to ensure that the signal was not saturated. Kinetic decays were observed by recording the variation in the laser-induced fluorescence (LIF) signal as a function of the time delay between the pulses from the photolysis and probe lasers. These traces of LIF signal *versus* time delay were fitted to single exponential functions, the fit being started at time delays sufficient to allow for rotational relaxation. This procedure yielded pseudo-first-order rate coefficients related to the rate of loss of CN radicals. Examples of typical decays at 123 K and at 298 K are shown in Fig. 3.

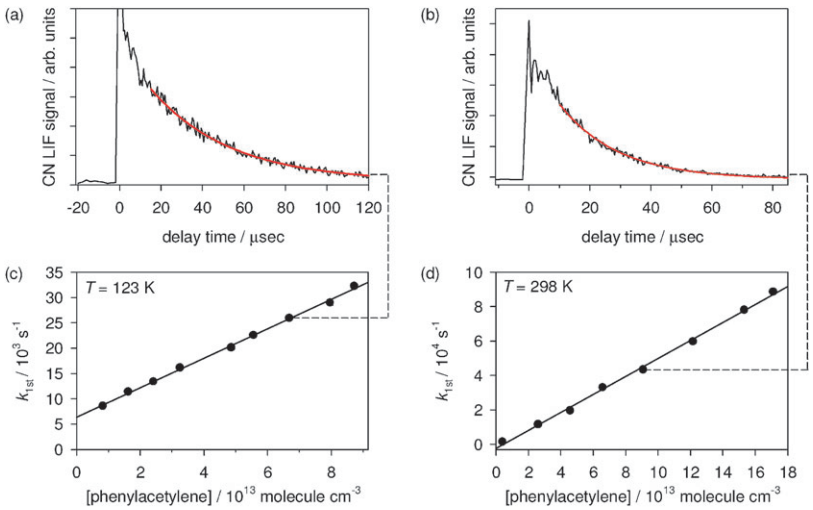

Fig. 3 The upper panels show the fitted decays of the laser-induced fluorescence from CN observed in mixtures containing (a) 6.68×10^{13} molecule cm^{-3} phenylacetylene at 123 K and a total density of 1.27×10^{17} molecule cm^{-3}, and (b) 9.39×10^{13} molecule cm^{-3} phenylacetylene at 298 K and a total density of 3.1×10^{16} molecule cm^{-3}. The lower panels show plots of the pseudo-first-order rate coefficients obtained from such experiments plotted against the concentration of phenylacetylene at (c) 123 K and (d) 298 K.

Phenylacetylene is a liquid at room temperature and atmospheric pressure. In order to introduce it at a known concentration into the CRESU flow, a heated bubbler system coupled to a temperature-controlled condenser was employed. Phenylacetylene (C_6H_5CCH, 98% purity, Sigma Aldrich) was placed in a round-bottomed flask held at ~320 K. A known flow of He (Air Liquide, ≥ 99.995% purity) was bubbled through the phenylacetylene, controlled by a calibrated mass flow controller (Tylan). This flow then passed through a condenser/heat exchanger consisting of a large number of small parallel tubes surrounded by water which was held at 298 K by a temperature controlled circulator.[33] This ensured the production of a flow of helium containing the saturated vapor pressure of phenylacetylene at 298 K. A 100 mbar pressure gauge (Edwards Barocel) monitored the pressure in the bubbler/heat exchanger and knowledge of this, coupled with the value of the saturated vapor pressure at 298 K (8.8 mbar) obtained by fitting the experimental data of Steele *et al.*[34] to Antoine's equation, enabled the calculation of the phenylacetylene flow for any given flow of He through the bubbler. The buffer gases (He, N_2, Air Liquide, ≥ 99.995% purity) were introduced into the reservoir on which was mounted the Laval nozzle *via* mass flow controllers (Tylan), and the known flow of phenylacetylene was mixed with this flow prior to the nozzle, enabling the introduction of a known concentration of phenylacetylene into the uniform supersonic flow.

2.3 Theoretical methods

The pathways of the title reaction on the adiabatic, ground state doublet surface were investigated theoretically. Multiple collision complexes were identified. Subsequently, probable low-energy isomerization and dissociation channels for each collision complex were searched for and characterized; these included hydrogen shifts, ring formation, ring opening, and hydrogen loss pathways. Finally, pathways for direct hydrogen abstractions by the cyano radical were also located. The optimized geometries and harmonic frequencies of the intermediates, transition states, and dissociation products were obtained at the level of the hybrid density functional theory, the unrestricted B3LYP/cc-pVTZ.[35] Their CCSD(T)/cc-pVDZ energies with B3LYP/cc-pVTZ zero-point energy corrections were computed.[36] The GAUSSIAN98 and 03 programs were employed in the electronic structure calculations.[37]

3. Results

3.1 Crossed beam experiments

In the cyano radical–phenylacetylene system, we monitored reactive scattering signal at mass-to-charge ratios of m/z = 127 ($C_9NH_5^+$) and m/z = 126 ($C_9NH_4^+$). The TOF spectra recorded at m/z ratio of 126 are identical to those obtained at m/z = 127 and could be fit with identical center-of-mass functions. This result demonstrates that signal at m/z = 126 originated from dissociative ionization of the C_9NH_5 reaction product in the electron impact ionizer of the detector. Fig. 4 depicts TOF spectra taken at m/z = 127 ($C_9NH_5^+$). Although this set of data alone suggests that in the reaction of the cyano radical with phenylacetylene, the cyano radical *versus* atomic hydrogen exchange channel is open, this information does not allow us to conclude if the hydrogen atom is lost from the

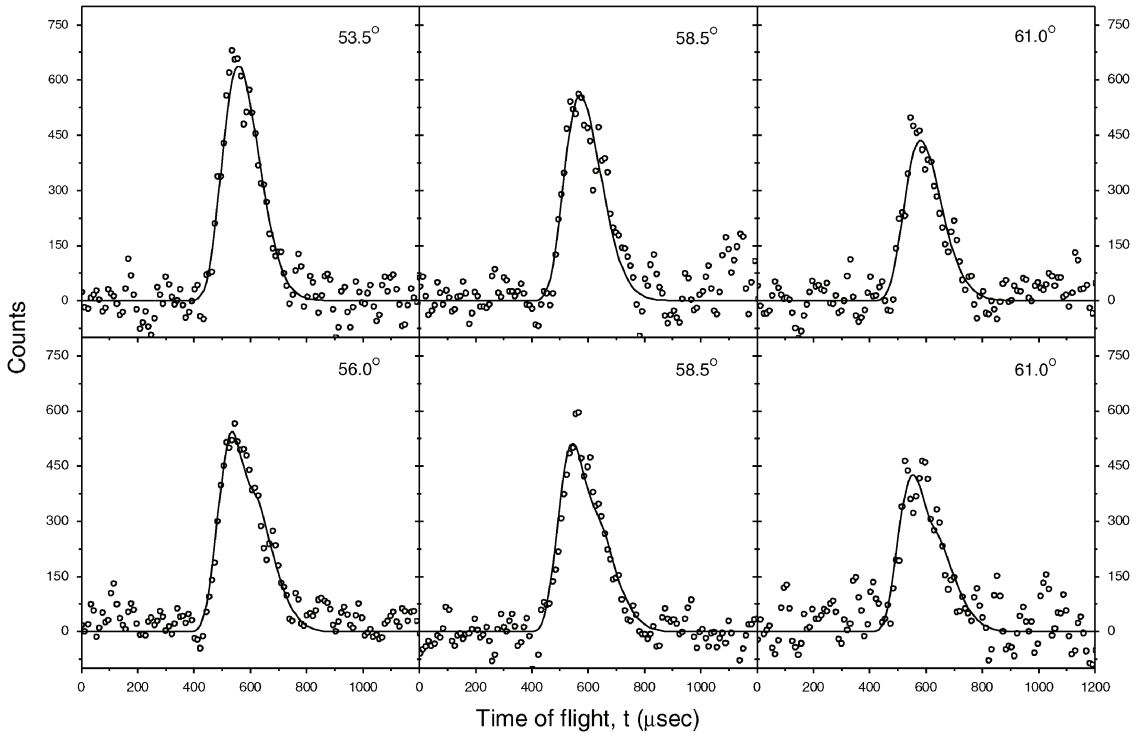

Fig. 4 Selected time-of-flight (TOF) data recorded at mass-to-charge ratios of m/z = 127 ($C_9NH_5^+$) (upper row) and 128 ($C_9NDH_4^+$) (lower row) of the reaction of cyano radicals with phenylacetylene and D_1-phenylacetylene at collision energies of 31.2 and 30.9 kJ mol^{-1}, respectively. The open circles are the experimental data, and the solid lines are the fits utilizing the best fit center-of-mass functions as depicted in Fig. 5.

phenyl ring or from the acetylenic group (or both). Therefore, we also conducted experiments with partially deuterated D_1-phenylacetylene, in which the acetylenic hydrogen atom was replaced by a deuterium atom. If the hydrogen atom is lost from the phenyl ring, we should observe signal at m/z = 128 ($C_9NDH_4^+$). Signal at m/z = 127 could either originate from dissociative ionization of the C_9NDH_4 to yield $C_9NDH_3^+$ or from a deuterium loss forming the C_9NH_5 product. By conducting the crossed beam experiment of cyano radical with D_1-phenylacetylene, we detected scattering signal at m/z = 128 ($C_9NDH_4^+$) and m/z = 127 ($C_9NDH_3^+$/$C_9NH_5^+$). As stated above, the TOF at m/z = 128 (Fig. 4) provided solid evidence that the hydrogen atom is ejected at least from the phenyl group. Since TOFs at m/z = 127 are—after scaling—superimposable to those at m/z = 128, we may conclude that within the detection limit of our system, the deuterium elimination channel is absent. The corresponding laboratory angular distributions obtained at m/z = 127 ($C_9NH_5^+$) and 128 ($C_9NDH_4^+$) from the reactions of the cyano radical with phenylacetylene and D_1-phenylacetylene, respectively, are shown in Fig. 5. Both distributions are spread about 30° in the scattering plane defined by both beams and peak close to the corresponding center-of-mass angles. It is very interesting to note that within the experimental errors, both laboratory angular distributions are overlapping. For completeness, we would like to mention that we also searched for reactive scattering signal originating from the *ipso* substitution of the ethynyl group by the cyano radical to yield cyano benzene (C_6H_5CN; m/z = 103). However, the ^{13}C isotopomer of inelastically scattered phenylacetylene resulted in a large background signal at m/z = 103; this made it impossible to identify the cyano *versus* ethynyl exchange pathway.

To extract information on the chemical dynamics, the laboratory data were transformed into the center-of-mass reference frame. Fits of the TOF data (Fig. 4) and of the laboratory angular distributions (Fig. 5) of signal m/z = 127 ($C_9NH_5^+$) and 128 ($C_9NDH_4^+$) from the reactions of the cyano radical with phenylacetylene and D_1-phenylacetylene could be fit with *identical* center-of-mass angular and translational energy distributions, *i.e.* a single channel fit yielding the reaction products of the molecular formula C_9NH_5 and C_9NDH_4 plus atomic hydrogen. For both systems, best fits of the center-of-mass translational energy distributions, $P(E_T)$s, were achieved with center-of-mass distributions extending to a maximum translational energy release, E_{max}, of 120 ± 18 kJ mol^{-1} (Fig. 6). Since the high energy cutoff resembles the sum of the absolute of the reaction energy and the collision energy, a subtraction of the collision energy from E_{max} helps to derive the reaction energies to be −89 ± 18 kJ mol^{-1}. Furthermore, the best fit $P(E_T)$ clearly peaks away from zero translational energy and exhibits a distribution maximum at about 15–25 kJ mol^{-1}. Our finding indicates that the exit transition state(s) is(are) likely to be tight.[28] By integrating the center-of-mass translational energy distribution and accounting for the available energy, we can also compute the average fraction of available energy channeling into the translational degrees of freedom; this results in a fraction of 42 ± 6%.

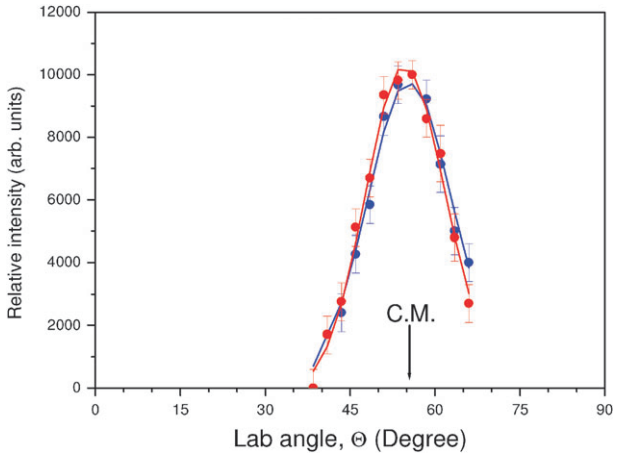

Fig. 5 Laboratory angular distributions of ion counts recorded at m/z = 127 ($C_9NH_5^+$, red) and 128 ($C_9NDH_4^+$, blue) in the reaction of the cyano radical with phenylacetylene and D_1-phenylacetylene at collision energies of 31.2 kJ mol^{-1} and 30.9 kJ mol^{-1}, respectively. The solid circles are the experimental data, and the solid lines the fits. C.M. defines the center-of-mass angle.

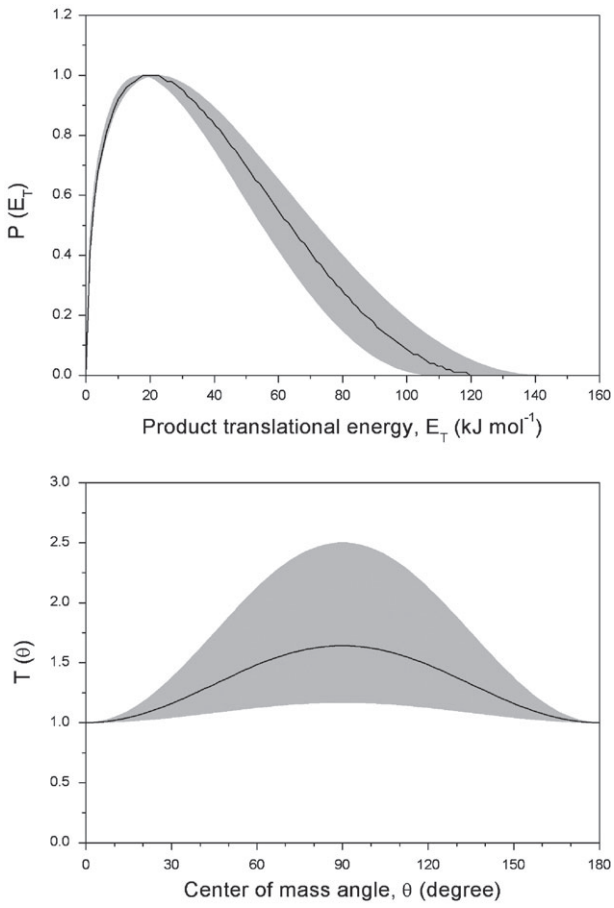

Fig. 6 Center-of-mass translational energy $P(E_T)$ (top) and angular $T(\theta)$ (bottom) distributions of the C_9NH_5 and C_9NDH_4 products formed in the reaction of the cyano radical with phenylacetylene and D_1-phenylacetylene. The hatched areas account for the experimental error limits of the laboratory angular distribution and the peak velocities of the reactant beams.

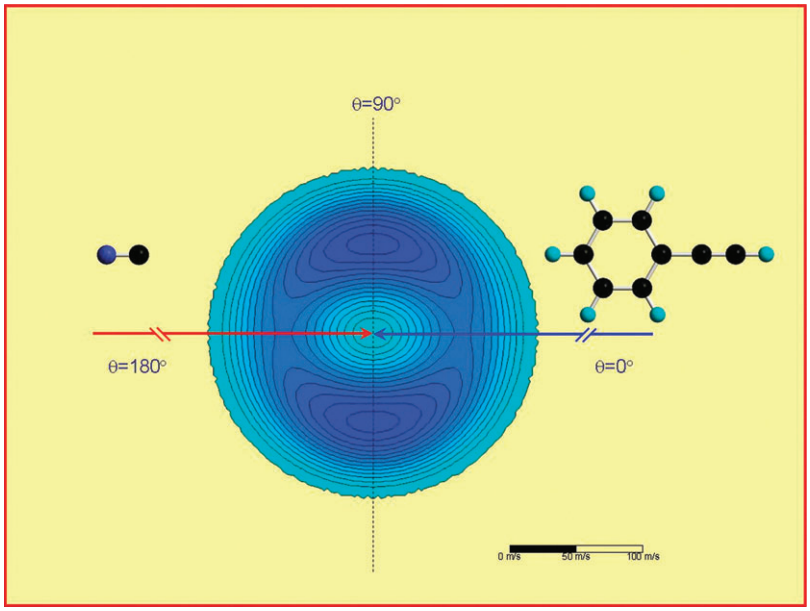

Fig. 7 Center-of-mass flux contour map distributions of the cyanophenylacetylene and D_1-cyanophenylacetylene products formed in the reaction of the cyano radical with phenylacetylene and D_1-phenylacetylene utilizing the best fit center-of-mass functions depicted in Fig. 4. The colors connect data points with an identical flux and range from dark blue (highest flux) to light blue (lowest flux). The units of axis are given in m s^{-1} (see legend).

Table 1 Experimental parameters for the kinetics experiments[a]

T/K	Carrier gas used, M	[M]/ 10^{16} molecule cm^{-3}	[Phenylacetylene]/ 10^{12} molecule cm^{-3}	No. of points	k/ 10^{-10} cm^3 molecule^{-1} s^{-1}
123	He	12.7	8.3–87.2	9	2.91 ± 0.31
200	N_2	5.6	6.8–61.0	9	4.38 ± 0.47
298	N_2	10.0	4.1–171.1	8	5.23 ± 0.58
298	N_2	3.1	40.7–181.0	8	5.22 ± 0.58
Weighted average at 298 K:					5.22 ± 0.41

[a] Uncertainties (here and throughout the table) are calculated using the standard error evaluated from the second order plot, multiplied by the appropriate Student's t factor for 95% confidence. An estimated systematic error of 10% was combined with this to yield the overall estimated uncertainty.

The derived center-of-mass angular distribution, $T(\theta)$, is shown in Fig. 6 and aids us to collect additional data on the reaction dynamics. The angular flux distribution depicts intensity over the complete angular range from 0° to 180° indicating that the reaction proceeds *via* indirect scattering dynamics through a reaction intermediate. Based on the best fit functions, the lifetime of this intermediate is—in both the cyanophenylacetylene and cyano–D_1-phenylacetylene systems—longer than its rotational period.[24] It is interesting to mention that best fits could be accomplished with a forward–backward symmetric $T(\theta)$ peaking at 90° with intensity ratios, $I(90°)/I(180°)$, of 1.5 ± 0.8 (sideways scattering). This polarization and the maximum at 90° strongly hints to geometrical constraints of the decomposing complex, *i.e.* a preferential hydrogen atom ejection *perpendicular* to the molecular plane of the rotating complex and almost *parallel* to the total angular momentum vector. This finding is also visible in the flux contour map (Fig. 7). It should be stressed that the fits of the laboratory angular distributions were significantly worse with isotropic (flat) angular distributions than those with distribution maxima at 90°.

3.2 Kinetics experiments

Second-order rate coefficients (k) for the reaction of $CN(X^2\Sigma^+)$ with phenylacetylene were obtained by measuring

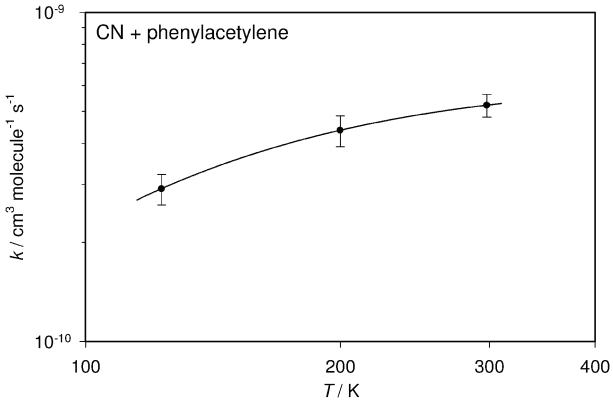

Fig. 8 Rate coefficients for the reaction of CN with phenylacetylene (●) as a function of temperature, displayed on a log–log scale. The solid line shows a fit to these data according to the modified Arrhenius equation (see text for details).

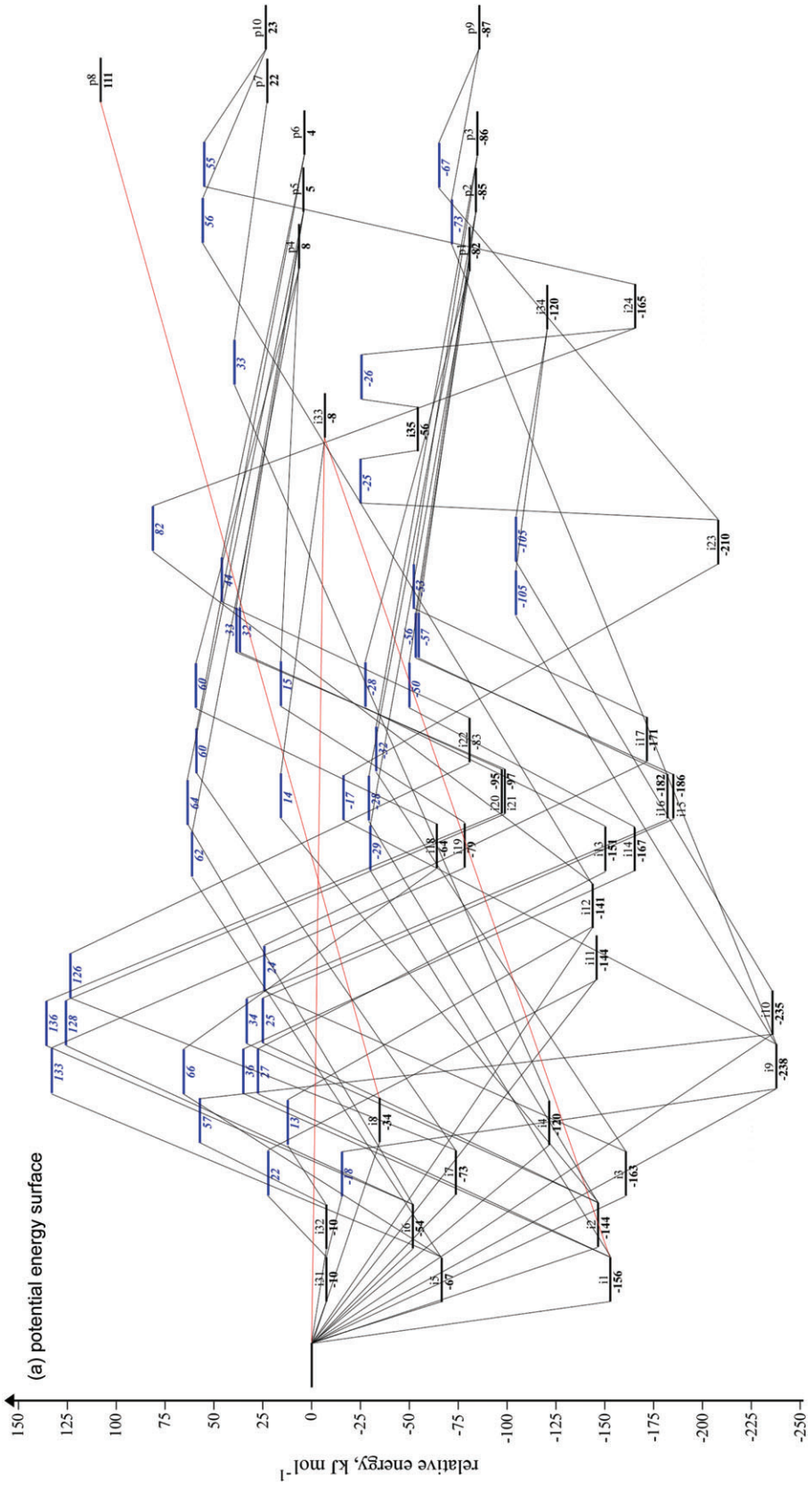

pseudo-first-order rate coefficients (k_{1st}) for the disappearance of the radical, by the methods described above, for several concentrations of phenylacetylene and then plotting k_{1st} against the concentration of phenylacetylene. The gradient of this line yields the value of k at the selected temperature. Two examples of these 'second-order plots' are shown in Fig. 3

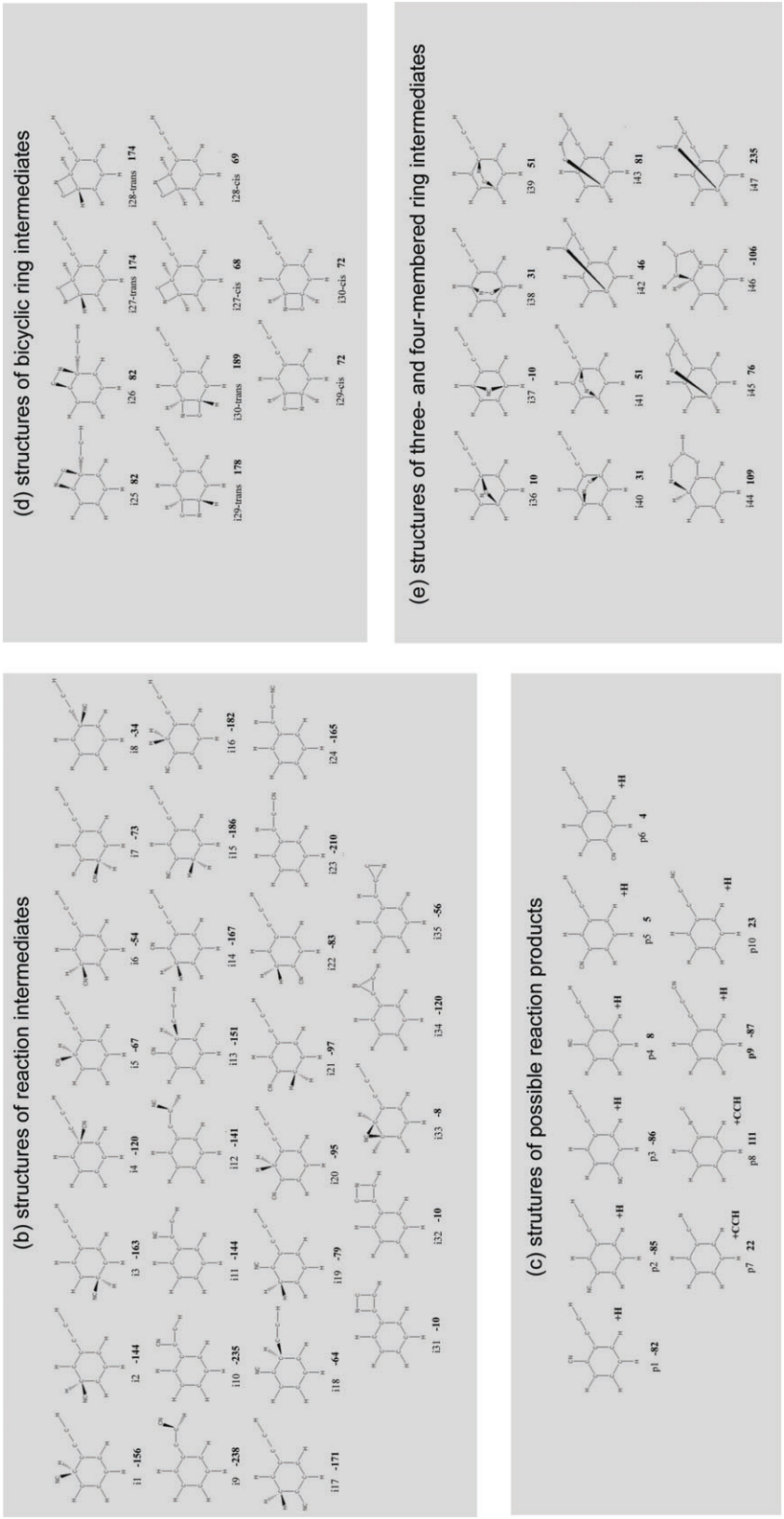

Fig. 9 Various sections of the potential energy surface relevant to the reaction of ground state cyano radicals with phenylacetylene under single collision conditions: (a) addition pathways of the cyano radical with its carbon or nitrogen atoms to a single carbon atom of the aromatic ring and acetylenic side chain, (b) structures of reaction intermediates, (c) structures of possible reaction products, (d) structures of energetically inaccessible bicyclic ring intermediates relevant to the migration of the cyano group over the carbon skeleton, and (e) structures of intermediates in which the cyano group is connected to two non-neighboring carbon atoms. Numbers in bold define the energies in kJ mol^{-1} with respect to the separated reactants.

at 123 and 298 K, respectively. Using different nozzles, measurements were made at temperatures of 123, 200, and 298 K. Room temperature measurements were performed by raising the pressure and reducing the gas flow to generate a subsonic flow at the same temperature as the reservoir.

The measured rate coefficients are summarized in Table 1 and displayed as a function of temperature on a log–log scale in Fig. 8. Standard errors from the second order plots have been multiplied by the appropriate Student's *t*-factor for 95% confidence limits. This corresponds to the statistical error. In addition, some systematic errors may have arisen from, for example, inaccuracies in the calibration of flow controllers and the determination of the phenylacetylene vapor flow or in the determination of the total gas density, but it is estimated that these errors are unlikely to exceed 10%. This estimate has been combined with the 95% confidence limits for statistical error and is shown in Table 1 and in Fig. 8. The rate coefficient displays a small positive temperature dependence. For modeling purposes, we recommend that a value of eqn (1) is used over the experimental temperature range, with mean 95% uncertainty limits of ±11%. This fit is shown as the line on Fig. 8.

$$k = 9.34 \times 10^{-10} (T/298\ \mathrm{K})^{-0.274} \exp[-173\ \mathrm{K}/T]\ \mathrm{cm}^3\ \mathrm{molecule}^{-1}\ \mathrm{s}^{-1} \quad (1)$$

Measurements were also carried out at lower temperatures from 23–83 K. However, in the course of these experiments a strong augmentation (up to an order of magnitude) of cyano radical LIF signal was observed on addition of phenylacetylene to the gas flow. Spectroscopic experiments demonstrated that this increased signal was indeed due to enhanced production and detection of cyano radicals in their ground state. A possible explanation could be that the large, polarizable phenylacetylene molecule can form a van der Waals complex with ICN at low temperatures. If this complex were to display an increased photodissociation cross-section and/or quantum yield to give $CN(X^2\Sigma^+)$ then this could explain the enhanced signal. Simulations using reasonable estimates of the formation rates of the complex show that, if this is the case, the measured rate coefficients could be artificially increased at these temperatures. It was therefore decided not to present these lower temperature results. It is to be emphasized that the results presented here showed no evidence whatsoever of this phenomenon of enhanced signal, which was only observed at 83 K and below.

3.3 Electronic structure calculations

The electronic structure calculations identified two principal pathways in the reaction of cyano radicals with phenylacetylene (Fig. 9 and 10). These are an initial barrier-less addition of the cyano radical with its carbon or nitrogen atom to the π electronic system of the benzene or acetylene units (Fig. 9) or the hydrogen abstraction channel (Fig. 10). Let us investigate these addition processes first (Fig. 9b). With its radical center located at the carbon atom, the cyano radical can add to the *ortho*, *meta*, *para*, or *ipso* position of the benzene ring leading to initial doublet collision complexes **i1**, **i2**, **i3**, and **i4**, respectively. These structures are stabilized by between 120 and 163 kJ mol^{-1} with respect to the separated reactants. Analogous addition steps with the nitrogen atom of the cyano radical result in the formation of four doublet isocyano intermediates **i5-i8**. Due to the weaker carbon–nitrogen bond formed, these structures are thermodynamically unfavorable compared to the nitrile radical intermediates **i1-i4** and stabilized by only 34 to 73 kJ mol^{-1} with respect to the cyano radical and phenylacetylene reactants. The cyano radical can also add with its carbon or nitrogen atom to the C1 or C2 atoms of the acetylene unit yielding collision complexes **i9-i12**; these intermediates are stabilized by 235–238 kJ mol^{-1} (cyano structures) and 144 kJ mol^{-1} (isocyano structures). Similarly to the ring addition intermediates, the isocyano structures are about 100 kJ mol^{-1} less stable than the corresponding cyano isomers.

What is the fate of these initial addition complexes? Our calculations identified three major reaction possibilities involving low lying C_9H_6N intermediates: (i) isomerization *via* hydrogen migration, (ii) rearrangements *via* migration of the cyano group involving bicyclic structures, and (iii) hydrogen atom elimination before and/or after isomerization (i and/or ii). All intermediates formed *via* addition to the aromatic ring (**i1-i8**) and to the acetylenic unit (**i9-i12**) can undergo hydrogen shifts. These hydrogen migrations involve significant barriers of 130–230 kJ mol^{-1} and yield ring-substituted cyano (**i13-i17**) and isocyano (**i18-i22**) intermediates as well as—*via* hydrogen migration at the acetylenic side group—intermediates **i23-i24** (Fig. 9b).

Besides the hydrogen shifts, the cyano groups can also migrate along the carbon skeleton of the initial collision complexes involving energetically high lying three- and four-membered reaction intermediates. Considering the

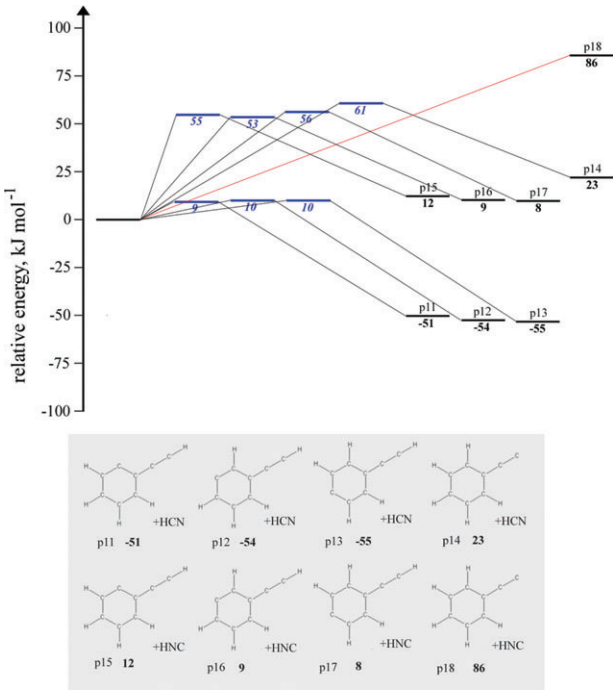

Fig. 10 Top: sections of the potential energy surface involved in hydrogen abstraction pathways. Bottom: structures of products formed in hydrogen abstraction processes.

four-membered ring intermediates, a 'formal' addition to two neighboring carbon atoms C1–C2, C2–C3, and C4–C5 of the ring leads to intermediates **i25-i26**, **i27-i28**, and **i29-i30** (Fig. 9d). Note that these structures can exist in their *cis* and *trans* forms with the *cis* forms being 100–110 kJ mol^{-1} more stable than the *trans* isomers. A formal addition to the acetylenic unit connects to the four-membered ring **i31** and **i32**. It should be stressed that all structures holding four-membered ring **i25-i30** are very high in energy and reside at least 68 kJ mol^{-1} above the energy of the separated reactants. Therefore, these are energetically not accessible at our collision energy, and we did not calculate the energies of the transition state connecting them. On the other hand, **i31-i32** are stabilized by about 10 kJ mol^{-1} compared to phenylacetylene and the cyano radicals and might be formed under bimolecular collision conditions and could be involved in cyano radical migrations at the acetylenic group. A search for possible three-membered ring as the result of a cyano group migration identified only one intermediate **i33** (formal addition to aromatic ring) and **i34** (formal addition to the acetylenic side group) (Fig. 9b). Alternative three-membered rings were found to break apart. Alternatively, **i35** connects **i23** and **i24**. Besides these 'traditional' , which were also characterized in the analogous reactions of cyano radicals with acetylene[23] and benzene,[22] we also found six in which the cyano group is formally connected *via* non-neighboring C1–C4 and C2–C5 carbon atoms in the aromatic ring leading to three-membered (**i36-i37**) and four-membered (**i38-i41**) ring (Fig. 9e). Finally, more exotic structures were characterized; here, the cyano group bridges a carbon atom from the aromatic ring with a carbon atom from the acetylenic unit, *i.e.* **i42-i47** (Fig. 9d).

Considering the reaction , multiple exit channels are possible. Here, we are discussing only those pathways which are energetically feasible under our experimental conditions. First, three energetically favorable *o*, *m*, and *p*-cyanophenylacetylene products **p1-p3** were located in which the cyano group formally replaces a hydrogen atom at the benzene ring. These products can be formed in overall exoergic reactions holding reaction energies of −82 to −86 kJ mol^{-1} from the initial collision complexes **i1-i3** and/or **i13-i17** formed *via* hydrogen shifts in **i1-i3** (Fig. 9c). In all cases, the exit transition states were found to be rather tight and located about 30–55 kJ mol^{-1} above the separated products. The overall formation of the analogous ring-substituted isocyano products (**p4-p6**) is weakly endoergic by 4–8 kJ mol^{-1} and also involves rather tight exit transition states placed 16–60 kJ mol^{-1} above the separated products. Note that the cyano *versus* ethynyl *ipso* substitutions yielding cyano benzene (**p7**) and isocyano benzene (**p8**) are endoergic by 22 and 111 kJ mol^{-1}, respectively. The cyano *versus* hydrogen exchange pathways at the acetylenic side chains form **p9** and **p10** *via* tight exit channels and holding overall reaction energies of −87 kJ mol^{-1} and 23 kJ mol^{-1}, respectively.

Finally, besides the indirect reaction pathways as discussed above, we also identified direct reaction mechanisms *via* hydrogen abstractions to form hydrogen cyanide (HCN) and hydrogen isocyanide (HNC) (Fig. 10). Eight direct abstraction pathways from the *o*, *m*, and *p* positions of the benzene ring and from the hydrogen atom connected to the C1 atom of the acetylenic side chains either with the carbon or nitrogen atom of the cyano radical were identified (**p11-p18**). Only the hydrogen abstractions from the *o*, *m*, and *p*-positions from the benzene ring leading to **p11-p13** were exoergic by 52–55 kJ mol^{-1}; the corresponding transition states are slightly higher by about 9 kJ mol^{-1} than the energy of the separated reactants.

4. Discussion

In the case of polyatomic reactions, it is very useful to combine the experimental data (crossed beam experiments and kinetics studies) with the electronic structure calculations. First, recall that the crossed beam experiment identified a molecule of the generic formula C_9NH_5 plus a light hydrogen atom as the reaction products. The reaction was also found to be exoergic by 89 ± 18 kJ mol^{-1} and involved a tight transition state located about 15–25 kJ mol^{-1} above the separated products. These data can be compared now with those obtained from our electronic structure calculations (Fig. 9). First, the experimentally derived reaction exoergicity correlates nicely with the ring-substitution products (**p1-p3**), but also with the acetylenic substitution product **p9**, in which the hydrogen atom is replaced by a cyano group. Within the error limits and based on the energetics alone, we cannot elucidate the branching ratios of these products. We shall also stress that the formation of these products involves tight exit transition states as predicted based on the center-of-mass translational energy distributions. Since the exit transition states to form the analogous isocyano products **p4-p6** and **p10** are located above the collision energy, we can safely assume that the formation of the isocyano products is energetically not feasible.

Having identified **p1-p3** and/or **p9** as feasible reaction products, we can now take a closer look at the results of the crossed beam reaction of D_1-phenylacetylene with cyano radicals. Here, we identified a C_9NDH_4 reaction product formed *via* the hydrogen atom *versus* cyano group exchange pathway. It is important to stress that the hydrogen exchange pathway could be only accessed *via* a hydrogen loss from the benzene ring. Therefore, we have to conclude that at least the aromatic ring substitution products **p1-p3** are formed. Further, it should be stressed that within the error limits, the laboratory angular distributions and derived center-of-mass functions of the hydrogen *versus* cyano radical exchange pathways were identical for both the phenylacetylene and D_1-phenylacetylene reactants. Therefore, based on these considerations, we may conclude that in case of the cyano plus phenylacetylene reaction—at least within the error limits—no hydrogen atoms were emitted from the acetylenic group. Consequently, based on the energetics *and* the comparison of the laboratory and center-of-mass functions derived for the cyanophenylacetylene and cyano–D_1-phenylacetylene systems, we can conclude that *o*, *m*, and *p*-cyanophenylacetylene (**p1-p3**) are the dominant reaction products.

What are the underlying reaction dynamics to form **p1-p3** under single collision conditions? We propose that the reaction follows indirect scattering dynamics *via* an addition of the cyano radical either with its radical center located at the

carbon atom or with its nitrogen atom to the *o*-, *m*-, and/or *p*-position at the benzene ring. These addition processes lead to **i1-i3** and **i5-i7**, respectively. Note that our electronic structure calculations predict that these addition processes have no entrance barrier. The barrier-less nature of the reaction is also supported by our low temperature kinetics studies. As discussed above, **i5-i7** cannot decay *via* atomic hydrogen loss to isonitriles, since the involved exit transition states are higher in energy than the collision energy. However, **i5-i7** can isomerize *via* bicyclic structures (Fig. 9) ultimately leading to thermodynamically favorable complexes **i1-i3**. Note that the larger cone of acceptance of the benzene ring, where the cyano group can add to five carbon atoms, compared to the acetylenic side chain (the cyano group can only add to the C1 atom), likely directs the attack of the electrophilic cyano group to the aromatic ring. Statistically speaking, the aromatic ring is favored by 5 : 1 compared to the acetylenic side chain. The collision complexes **i1-i3** can either decompose *via* atomic hydrogen elimination to yield *o*-, *m*-, and *p*-cyanophenylacetylene (**p1-p3**) *via* tight exit transition states or undergo hydrogen migration to **i13-i17** prior to atomic hydrogen loss yielding **p1-p3**. Our statistical calculations utilized the Rice–Ramsperger–Kassel–Marcus (RRKM) approach[38] and suggest that only a minor fraction of 0.003%, 0.006%, 0.012% of **p1-p3**, respectively, undergo hydrogen migration prior to instantaneous hydrogen elimination. It should be stressed that due to the small differences in energetics of **p1-p3** we cannot experimentally separate their relative contributions. Recall that best fits could be accomplished with a forward–backward symmetric $T(\theta)$ peaking at 90° with intensity ratios, $I(90°)/I(180°)$, of 1.5 ± 0.8 (sideways scattering). This polarization and the maximum at 90° strongly point to geometrical constraints of the decomposing complex, *i.e.* a preferential hydrogen atom ejection *perpendicular* to the molecular plane of the rotating complex. The structures of the transition states involved in the decomposition of **i1-i3** to **p1-p3** are depicted in Fig. 11. These computational results correlate very nicely with the derived center-of-mass angular distribution. In all , the hydrogen atom was found to leave at an angle of around 90° with respect to the molecular plane of the decomposing complex. It is interesting to note that the derived reaction dynamics are similar to those found in the reaction of cyano radicals with benzene and D_6-benzene at collision energies between 19.5 and 34.4 kJ mol^{-1} to form the cyanobenzene and D_5-cyanobenzene products.[22] Here, the reaction dynamics were indirect, involved the barrier-less addition of the cyano radical to the benzene molecule, and exposed center-of-mass angular distributions peaking at 90°. Theory predicted a H–C–C angle of 101.2° in the exit transition state. The reaction was found to be exoergic by 80–95 kJ mol^{-1}.

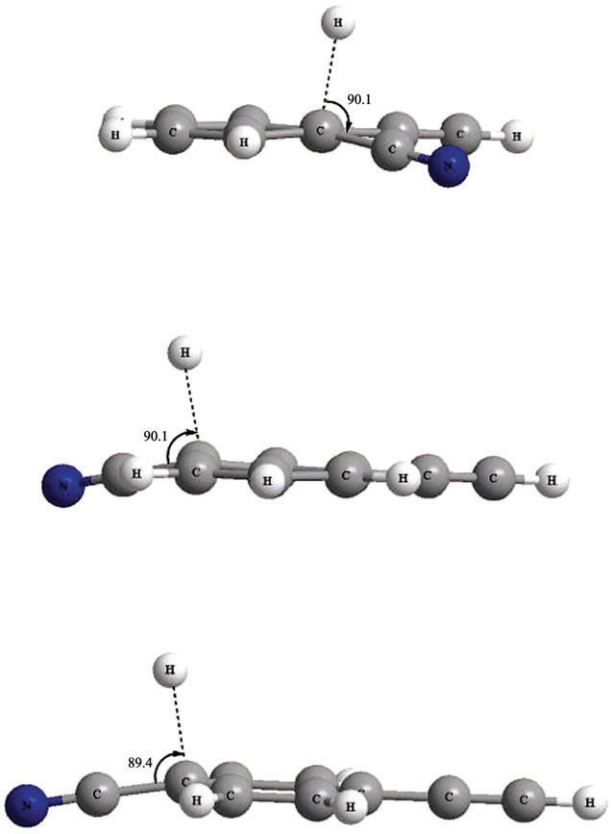

Fig. 11 Side view of the structures of transition states involved in the decomposition of **i1-i3** to **p1-p3** (from top to bottom); angles are given in degrees.

5. Summary

The chemical reaction dynamics to form *o*-, *m*-, and *p*-cyanophenylacetylene *via* the neutral–neutral reaction of ground state cyano radicals with phenylacetylene and D_1-phenylacetylene were investigated in crossed beam experiments at collision energies of 31.2 and 30.9 kJ mol^{-1}, respectively. These studies were combined with kinetics measurements of the rate coefficients at temperatures of 123, 200, and 298 K and with electronic structure calculations. Forward-convolution fitting of our experimental data together with the electronic structure calculations and the kinetics studies indicate that the reaction has no entrance barrier and is governed by an initial attack of the electrophilic cyano radical *via* its carbon and/or nitrogen atom to form **i1-i3** and **i5-i7**, respectively. The latter can isomerize *via* bicyclic structures yielding eventually **i1-i3**. The **i1-i3** fragmented almost exclusively *via* atomic hydrogen elimination to yield *o*-, *m*-, and *p*-cyanophenylacetylene (**p1-p3**) *via* tight exit transition states. Similar to the related reaction of cyano radicals with benzene, the hydrogen atom was found to be emitted almost perpendicularly to the molecular plane of the rotating complex. The overall reaction to form *o*-, *m*-, and *p*-cyanophenylacetylene was found to be exoergic by 89 ± 18 kJ mol^{-1} in nice agreement with the calculations. Isocyano products were not formed. Likewise, under the low temperature conditions on Titan and in the kinetics experiments, the direct hydrogen abstraction pathways are closed due to an inherent barrier to reaction. In summary, our combined dynamics, kinetics and theoretical study identified the reaction mechanism to form *o*-, *m*-, and *p*-cyanophenylacetylene (**p1-p3**) in the crossed beams experiments and also in the atmosphere of Saturn's moon Titan. The *o*-cyanophenylacetylene isomer is of particular relevance as a potential building block to the formation of

nitrogen-substituted didehydronaphthalene molecules in analogy to didehydronaphthalene (Fig. 1) in Titan's aerosol layers—a pathway hitherto neglected by the planetary science modeling community. The provision of the rate coefficients and the reaction products—two crucial prerequisites in chemical reaction networks modeling the atmospheric chemistry of Saturn's moon Titan—should trigger an in-depth analysis of the role of this system toward the formation of nitrogen substituted PAHs in Titan's aerosol layers.

Acknowledgements

This work was supported by the US National Science Foundation 'Collaborative Research in Chemistry Program' (NSF-CRC; CHE-0627854). The Rennes authors also wish to thank the *Programme National de Planétologie*, the *Programme National Physique et Chimie du Milieu Interstellaire*, the *Région de Bretagne* and *Rennes Métropole* for support.

References

1 M. Frenklach, *Phys. Chem. Chem. Phys.*, 2002, **4**, 2028–2037.
2 A. Tielens, *Annu. Rev. Astron. Astrophys.*, 2008, **46**, 289.
3 I. W. M. Smith, E. Herbst and Q. Chang, *Mon. Not. R. Astron. Soc.*, 2004, **350**, 323–330.
4 F. Goulay and S. R. Leone, *J. Phys. Chem. A*, 2006, **110**, 1875–1880.
5 N. Sarker, A. Somogyi, J. I. Lunine and M. A. Smith, *Astrobiology*, 2003, **3**, 719–726.
6 R. A. Kerr, *Science*, 2005, **307**, 330–331.
7 E. Wilson, *Chem. Eng. News*, 2005, **83**, 6.
8 F. Raulin, P. Coll, Y. Benilan, P. Bruston, M.-C. Gazeau, P. Paillous, N. Smith, R. Sternberg, D. Coscia and G. Israel, *Exobiology: Matter, Energy, and Information in the Origin and Evolution of Life in the Universe*, Kluwer Academic Publishers, Dordrecht, 1998.
9 C. P. McKay, A. Coustenis, R. E. Samuelson, M. T. Lemmon, R. D. Lorenz, M. Cabane, P. Rannou and P. Drossart, *Planet. Space Sci.*, 2001, **49**, 79–99.
10 P. Coll, D. Coscia, N. Smith, M. C. Gazeau, S. I. Ramirez, G. Cernogora, G. Israel and F. Raulin, *Planet. Space Sci.*, 1999, **47**, 1331–1340.
11 C. A. Griffith, T. Owen, G. A. Miller and T. Geballe, *Nature*, 1998, **395**, 575–578.
12 L. M. Lara, E. Lellouch and V. Shematovich, *Astron. Astrophys.*, 1999, **341**, 312–317.
13 A. Marten, T. Hidayat, Y. Biraud and R. Moreno, *Icarus*, 2002, **158**, 532–544.
14 E. H. Wilson and S. K. Atreya, *Planet. Space Sci.*, 2003, **51**, 1017–1033.
15 B. N. Tran, M. Force, R. G. Briggs, J. P. Ferris, P. Persans and J. J. Chera, *Icarus*, 2008, **193**, 224–232.
16 N. A. Teanby, P. G. J. Irwin, R. de Kok, A. Jolly, B. Bézard, C. A. Nixon and S. B. Calcutt, *Icarus*, 2009, **202**, 620–631.
17 R. I. Kaiser and N. Balucani, *Acc. Chem. Res.*, 2001, **34**, 699–706; X. Gu, F. Zhang and R. I. Kaiser, *J. Phys. Chem. A*, 2008, **112**, 9607–9613; F. Zhang, S. Kim, R. I. Kaiser and A. M. Mebel, *J. Chem. Phys.*, 2009, **130**, 234308.
18 I. R. Sims, J.-L. Queffelec, D. Travers, B. R. Rowe, L. B. Herbert, J. Karthaeuser and I. W. M. Smith, *Chem. Phys. Lett.*, 1993, **211**, 461–468.
19 D. Carty, V. Le Page, I. R. Sims and I. W. M. Smith, *Chem. Phys. Lett.*, 2001, **344**, 310.
20 A. M. Mebel, V. V. Kislov and R. I. Kaiser, *J. Am. Chem. Soc.*, 2008, **130**, 13618–13629.
21 M. Frenklach and H. Wang, in: *Soot formation in combustion: mechanisms and models*, ed. H. Bockhorn, Springer-Verlag, Berlin, 1994, pp. 162–192; M. Frenklach, *Phys. Chem. Chem. Phys.*, 2002, **4**, 2028–2037.
22 N. Balucani, O. Asvany, A. H. H. Chang, S. H. Lin, Y. T. Lee, R. I. Kaiser, H. F. Bettinger, P. v. R. Schleyer and H. F. Schaefer III, *J. Chem. Phys.*, 1999, **111**, 7457–7471.
23 L. C. L. Huang, Y. T. Lee and R. I. Kaiser, *J. Chem. Phys.*, 1999, **110**, 7119–7122.
24 X. Gu, Y. Guo, F. Zhang, A. M. Mebel and R. I. Kaiser, *Faraday Discuss.*, 2006, **133**, 245–275.
25 R. I. Kaiser, J. Ting, L. C. L. Huang, N. Balucani, O. Asvany, Y. T. Lee, H. Chan, D. Stranges and D. Gee, *Rev. Sci. Instrum.*, 1999, **70**, 4185–4191.
26 Y. Guo, X. Gu, F. Zhang, A. M. Mebel and R. I. Kaiser, *Phys. Chem. Chem. Phys.*, 2007, **9**, 1972–1979; X. Gu, Y. Guo, A. M. Mebel and R. I. Kaiser, *Chem. Phys. Lett.*, 2007, **449**, 44–52.
27 M. Vernon, Ph.D. Thesis, University of California, Berkeley, 1981; M. S. Weiss, Ph.D. Thesis, University of California, Berkeley, 1986.
28 R. D. Levine, *Molecular Reaction Dynamics*, Cambridge University Press, Cambridge, UK, 2005.
29 I. R. Sims, J. L. Queffelec, A. Defrance, C. Rebrion-Rowe, D. Travers, B. R. Rowe and I. W. M. Smith, *J. Chem. Phys.*, 1992, **97**, 8798.
30 I. R. Sims, J. L. Queffelec, A. Defrance, C. Rebrion-Rowe, D. Travers, P. Bocherel, B. R. Rowe and I. W. M. Smith, *J. Chem. Phys.*, 1994, **100**, 4229.
31 G. Dupeyrat, J. B. Marquette and B. R. Rowe, *Phys. Fluids*, 1985, **28**, 1273.
32 W. H. Fisher, R. Eng, T. Carrington, C. H. Dugan, S. V. Filseth and C. M. Sadowski, *Chem. Phys.*, 1984, **89**, 457.
33 S. Hamon, S. D. Le Picard, A. Canosa, B. R. Rowe and I. W. M. Smith, *J. Chem. Phys.*, 2000, **112**, 4506.
34 W. V. Steele, R. D. Chirico, S. E. Knipmeyer and A. Nguyen, *J. Chem. Eng. Data*, 2002, **47**, 689.
35 A. D. Becke, *J. Chem. Phys.*, 1993, **98**, 5648–5652; A. D. Becke, *J. Chem. Phys.*, 1992, **96**, 2155–2160; A. D. Becke, *J. Chem. Phys.*, 1992, **97**, 9173–9177; C. Lee, W. Yang and R. G. Parr, *Phys. Rev. B: Condens. Matter*, 1988, **37**, 785–789.
36 G. D. Purvis and R. J. Bartlett, *J. Chem. Phys.*, 1982, **76**, 1910–1918; C. Hampel, K. A. Peterson and H.-J. Werner, *Chem. Phys. Lett.*, 1992, **190**, 1–12; P. J. Knowles, C. Hampel and H.-J. Werner, *J. Chem. Phys.*, 1993, **99**, 5219–5227; M. J. O. Deegan and P. J. Knowles, *Chem. Phys. Lett.*, 1994, **227**, 321–326.
37 M. J. Frisch, G. W. Trucks, H. B. Schlegel, G. E. Scuseria, M. A. Robb, J. R. Cheeseman, J. A. Montgomery, Jr., T. Vreven, K. N. Kudin, J. C. Burant, J. M. Millam, S. S. Iyengar, J. Tomasi, V. Barone, B. Mennucci, M. Cossi, G. Scalmani, N. Rega, G. A. Petersson, H. Nakatsuji, M. Hada, M. Ehara, K. Toyota, R. Fukuda, J. Hasegawa, M. Ishida, T. Nakajima, Y. Honda, O. Kitao, H. Nakai, M. Klene, X. Li, J. E. Knox, H. P. Hratchian, J. B. Cross, V. Bakken, C. Adamo, J. Jaramillo, R. Gomperts, R. E. Stratmann, O. Yazyev, A. J. Austin, R. Cammi, C. Pomelli, J. W. Ochterski, P. Y. Ayala, K. Morokuma, G. A. Voth, P. Salvador, J. J. Dannenberg, V. G. Zakrzewski, S. Dapprich, A. D. Daniels, M. C. Strain, O. Farkas, D. K. Malick, A. D. Rabuck, K. Raghavachari, J. B. Foresman, J. V. Ortiz, Q. Cui, A. G. Baboul, S. Clifford, J. Cioslowski, B. B. Stefanov, G. Liu, A. Liashenko, P. Piskorz, I. Komaromi, R. L. Martin, D. J. Fox, T. Keith, M. A. Al-Laham, C. Y. Peng, A. Nanayakkara, M. Challacombe, P. M. W. Gill, B. Johnson, W. Chen, M. W. Wong, C. Gonzalez and J. A. Pople, *GAUSSIAN 03 (Revision C.02)*, Gaussian, Inc., Wallingford, CT, 2004.
38 J. I. Steinfeld, J. S. Francisco and W. L. Hase, *Chemical Kinetics Dynamics*, Prentice Hall, Engelwood Cliffs, NJ, 2nd edn, 1999.